Beni-Suef University Journal of Basic and Applied Sciences

RESEARCH

Open Access

Alleviative effect of betaine against copper oxide nanoparticles-induced hepatotoxicity in adult male albino rats: histopathological, biochemical, and molecular studies

Asmaa R. Hashim[1*], Dina W. Bashir[1], Eman. Rashad[1], Mona K. Galal[2], Maha M. Rashad[2], Nasrallah M. Deraz[3], Elsayed A. Drweesh[4] and S. M. El-Gharbawy[1]

Abstract

Background Copper oxide nanoparticles (CuO-NPs) have gained interest due to their availability, efficiency, and their cost-effectiveness. Betaine is an essential methyl donor and takes part in various physiological activities inside the body; it is found to have protective and curative effects against various liver diseases. The present study aimed to evaluate the hepatotoxic effect of CuO-NPs on adult male albino rats and the ability of betaine to alleviate such hepatotoxicity.

Methods Forty adult male albino Wister rats were grouped into 4 groups (10 rats/group): group I a negative control, group II (CuO-NPs) injected with CuO-NPs intra peritoneal by insulin needle (0.5 mg/kg/day), group III (betaine + CuO-NPs) administered betaine orally by gavage needle (250 mg/kg/day 1 h before CuO-NPs) and CuO-NPs (0.5 mg/kg/day) finally, group IV (betaine) administered betaine orally by gavage needle (250 mg/kg/day) for consecutive 28 days. Blood and liver samples were gathered and processed for biochemical, molecular, histopathological, and immunohistochemical investigations.

Results Group II displayed a marked rise in alanine aminotransferase (ALT), aspartate aminotransferase (AST), and malondialdehyde (MDA) levels. Furthermore, there is an excessive upregulation of the inflammatory biomarkers interleukin1 beta (IL-1β) and tumor necrosis factor-alpha (TNF-α). On the other hand, substantial reduction in glutathione (GSH) levels and significant downregulation at glutathione peroxidase (GPx) mRNA gene expression. Regarding the histopathological deviations, there were severe congestion, dilatation and hyalinization of blood vessels, steatosis, hydropic degeneration, hepatocytic necrosis, increased binucleation, degenerated bile ducts, hyperplasia of ducts epithelial lining, and inflammatory cells infiltration. Immunohistochemically, there was a pronounced immunoreactivity toward IL-1β. Luckily, the pre-administration of betaine was able to mitigate these changes. MDA was dramatically reduced, resulting in the downregulation of IL-1β and TNF-α. Additionally, there was a considerable rise in GSH levels and an upregulation of GPx. Histopathological deviations were substantially improved as diminished dilatation, hyalinization and congestion of blood vessels, hepatocytes, and bile ducts are normal to some extent. In addition, IL-1β immunohistochemical analysis revealed marked decreased intensity.

*Correspondence:
Asmaa R. Hashim
asmaarabea@cu.edu.eg
Full list of author information is available at the end of the article

Conclusion Betaine can effectively reduce the hepatotoxicity caused by CuO-NPs via its antioxidant properties and its ability to stimulate the cell redox system.

Keywords Copper oxide nanoparticles, Betaine, Liver, Malondialdehyde, Interleukin, Histopathology, Steatosis

1 Background

In the twenty-first century, a new term called nanoparticles (NPs) has been introduced, attracting the interest of industry and chemistry scientists due to their unique characteristics [1]. However, NPs characterized by their minute sizes ranging from 1 to 100 nm have larger surface areas [2]. So, they are used in a wide range of fields, which in turn opens up new horizons in the fields of industry and technology [3]. As the rule of life is that everything has advantages and disadvantages, the high use of NPs causes the world to fall into many challenges [3].

Metal-oxide NPs, including heavy metal ions, are characterized by their unique shape, aggregation properties, and surface structure, enabling them to be suitable for applications in various industries [4]. The most commonly used of those metal-oxide NPs is copper oxide nanoparticles (CuO-NPs) [5]. CuO-NPs have gotten a lot of attention due to their distinctive benefits and characteristics [6].

Owing to their outstanding thermophysical properties, CuO-NPs are valuable in several applications in the electronics technology field, such as electronic chips, semiconductors, heat transfer systems, and metal catalyst [7]. Moreover, they are beneficial in the pharmacological field particularly, in the anti-microbial production and prevention of diseases caused by methicillin-resistant *Staphylococcus aureus* (MRSA) and *Escherichia coli* (*E. coli*) [8]. CuO-NPs are also used in poultry and livestock production as feed additives and in the metallic coating industry for the production of lubricants and plastics [9].

As CuO-NPs have excellent biocidal activity, they are used in water filters and antifouling paint effectively, but this biocidal activity may be threatening to all living creatures and the environment, so it was classified as an environmental pollutant [10]. The widespread use of CuO-NPs led to environmental release and contamination; thus, people are exposed to them through a variety of sources, including effluents, leaks during shipping and administration, as well as the inappropriate handling of raw materials and disposal [9]. These NPs access the body by inhalation, oral, and dermal routes [11].

CuO-NPs overload can stimulate hepatic, gastrointestinal, renal, splenic, and neuronal disorders in rats via depletion of body antioxidants, reactive oxygen species (ROS) generation, and deoxyribonucleic acid (DNA) damage [12, 13]. Oxidative stress initiated by CuO-NPs is always associated with inflammatory reactions and undesirable effects on the process of drug metabolism, which is accomplished in the liver by inhibiting the expression of cytochrome P450 (CYP450) enzymes, so increasing drug-drug interactions risk [14]. CuO-NPs, like other NPs are characterized by their smaller sizes than cellular organelles, so they can penetrate the basic biological membranes easily, interact with living cells and tissues, and alter their basic functions [15].

Exposure to CuO-NPs induces the elevation of different oxidative stress markers [16, 17], raising the intracellular enzymes activities as transaminases and alkaline phosphatase (ALP), causing cellular leakage and loss of cell membrane functional integrity [18], and histopathological deviations in several organs, including the liver [9, 19].

Owing to the continuous modifications in people's living habits and environment, the number of those suffering from liver disease increases annually worldwide [20]. As the liver (the largest digestive gland) is the most commonly targeted organ for cytotoxicity due to its unique role in storage and energy metabolism, and it is the principal site for various biotransformation reactions [21]. Therefore, the liver is more likely to be affected by CuO-NPs intoxication [9].

Betaine (trimethylglycine) is a type of water-soluble alkaloid quaternary amine that usually exists in different foods, such as wheat germ, spinach, sugar beet, wolfberry, and shrimp [22]. It is regarded as a lipotropic agent and significantly contributes to the transmethylation pathway, forming S-adenosylmethionine (SAM) and phosphatidylcholine. The latter is vital for maintaining cell membrane integrity. Therefore, it affects transmembrane signaling, cholinergic neurotransmission, and lipid metabolism [23].

Previous reports have indicated that betaine has its anti-inflammatory effect via inhibition of reactive species (RS) production and modulation of the ratio of reduced glutathione (GSH) to oxidized glutathione (GSSG) [24]. It diminishes the possibility of inflammation through inhibition of tumor necrosis factor alpha (TNFα) and interleukin-6 (IL-6) expression [22]. Betaine is regarded as a cytoprotective agent in various organs, including the liver [25]. It has previously been used in the treatment of liver diseases such as liver cirrhosis and necrosis caused by carbon tetra chloride (CCl4) [26].

Recently, hepatic disease has become one of the most prevalent diseases worldwide, and the increasing use of

hepatotoxic NPs, including CuO-NPs, should be minimized [27]. Therefore, searching for alternative agents instead of drugs should be taken into consideration. Betaine is a naturally existing, available substance and there is a scarcity in using betaine against CuO-NPs. For these reasons, this research turned attention toward the betaine protective effect against CuO-NPs hepatotoxicity. Our main objective of this study is to investigate the hepatotoxicity of CuO-NPs and the ability of betaine to alleviate this toxicity at histopathological, immunohistochemical, biochemical, and molecular levels in the liver of adult male albino rats.

2 Methods

2.1 Chemicals and reagents

Betaine $C_5H_{11}NO_2$, Amargain industrial complex (Opp.S.T. stand, LBS, marg, Khopat Thane Mumbai, Maharashtra, India) was purchased from El-Mekkawy Company, Cairo, Egypt.

Copper (II) nitrate trihydrate with the linear formula Cu $(NO_3)_2{\cdot}3H_2O$ as a chemical material from Sigma-Aldrich Company (Darmstadt, Taufkirchen, Germany) was used without further refining. Raw egg white from surrounding chickens was used without drying or any further purification.

All chemicals and reagents used were of analytical grade.

2.2 Preparation route of CuO-NPs

In a glass beaker, about 2.43 g of Cu $(NO_3)_2{\cdot}3H_2O$ was mixed well with 10 ml of egg white until the formation of a homogeneous precursor. The precursor was gently heated on a hot plate for 5 min., and then, the heat of treatment increased gradually until it reached 300 °C within 10 min. It was noted that the crystal water underwent a smooth process of vaporization, resulting in the generation of a significant amount of foam through convection. At a temperature of 300 °C, a spark spontaneously erupted on one edge of the beaker and rapidly spread across the entire mass, resulting in the formation of a chunky and voluminous substance inside the beaker. The product has been transferred into agate mortar and ground to obtain a very fine powder. The fine powder was finally transferred to a porcelain crucible and laid into a muffle at 700 °C for 2 h for calcination.

2.3 Instrumentation

Fourier-transform infrared (FTIR) spectra were recorded on a Nicolet iS10, Thermo-Fisher Scientific, USA, using a KBr pellet. X-ray diffraction (XRD) analysis of distinctly mixed solids was performed on an XRD instrument from the Bruker AXS D8 advance diffractometer (Bruker, Karlsruhe, Germany) using Cu Kα radiation ($\lambda = 1.5406$ Å) under 40 kV and 40 mA. The crystallite size of CuO present in the investigated solid was calculated using Scherrer equation based on XRD line broadening [28].

$$d = \frac{B\lambda}{\beta \cos\theta}$$

where d is the average crystallite size of the phase being studied, B is the Scherrer constant (0.89), λ is the wavelength of the X-ray beam being employed, β is the full-width half maximum (FWHM) of diffraction, and θ is the Bragg's angle. The Raman shift of the samples was collected on an I-Raman Plus 532S portable laser Raman spectrometer conducted with a BAC151C Raman Video Micro-sampling System (B&W TEK, USA) and 20–100× lenses. The micrographs of CuO-NPs were performed by transmission electron microscopy (TEM) using JEOL JAX-840A and JEOL model 1230 (JEOL, Tokyo, Japan) at an operating voltage of 25 and 100 keV, respectively. It was performed by drop-coating the ethanol suspension of the synthesized CuO onto carbon-coated copper grids (40 μm × 40 μm mesh size). The samples were then dried and kept under a vacuum prior to being loaded into a specimen holder. The average diameter, size-distribution analysis, and zeta potential(ZP) were performed on aqueous sample suspensions using a Zeta Sizer (ZS), a ZS-Nano instrument, from Malvern Instruments Ltd. (Malvern, UK). For ZP measurements, the sample was dispersed in water and sonicated for 30–60 min. prior to assessment.

2.4 Animal grouping and experimental design

2.4.1 Experimental animals and ethical approval

Forty adult male Wistar albino rats (180–200 g, 4–5 months) were obtained from VACSERA animal house, Abasia, Egypt. Rats were maintained in polypropylene cages under similar environmental laboratory conditions (temperature, relative humidity, and lighting). They were fed a well-adjusted and balanced diet as well as free access to distilled water. All animals were treated and cared for humanely. The protocol was ethically adopted by the Faculty of Veterinary Medicine at Cairo University's Institutional Animal Care and Use Committee (IACUC) (protocol no. Vet CU 03162023754).

2.4.2 Experimental design

After 2 weeks of acclimation period, rats were randomly grouped into four groups ($n = 10$, 5 animals per cage) for 28 consecutive days according to the dietary treatments. Group I (negative control); served as the untreated negative control group and was nourished with a balanced diet and pure distilled water. Group II (CuO-NPs-exposed

group); rats were daily intraperitoneally injected with CuO-NPs dissolved in saline (0.5 mg/kg body weight/day) by insulin needle according to Mohamed Mowafy et al. [29]. Group III (betaine plus CuO-NPs) received daily betaine dissolved in saline orally by gavage needle (250 mg/kg body weight/day) according to Abdel-Daim and Abdellatief [30], then one hour later intraperitoneally injected with CuO-NPs (0.5 mg/kg body weight/day) by insulin needle. Group IV (betaine) received daily only betaine orally by gavage needle (250 mg/kg body weight/day).

2.5 Sample collection and preparation

Finally, at the end of the experimental period before blood sampling, animals were inhaled with 2% isoflurane. Blood samples were collected from the retro-orbital venous plexus without an anticoagulant. Then centrifugation of these blood samples at 3000 rpm for 10 min for separation of the serum. Later on, serum was stored at − 20 °C for liver function assessment. Then cervical decapitation for all animals and liver samples were collected. A part of these obtained liver samples was stored at − 80 °C for evaluation of oxidative stress markers and analysis of quantitative real-time polymerase chain reaction (qRT-PCR). The remaining part of the collected liver samples was kept in a 10% neutral-buffered formalin solution (10% NBF) for histopathological and immunohistochemical examinations.

2.6 Biochemical investigation

2.6.1 Liver function test (liver biomarkers)

Assessment of serum alanine aminotransferase (ALT) and aspartate aminotransferase (AST) activities was performed using commercial reagent kits following the provided instructions (Bio-diagnostic Co., Giza, Egypt).

2.6.2 Oxidative stress biomarkers

Reduced glutathione (GSH) and malondialdehyde (MDA) levels were determined in hepatic tissue homogenates using colorimetric kits purchased from Bio-diagnostic Co., Giza, Egypt, following the manufacturer's instructions.

2.6.3 qRT-PCR analysis for glutathione peroxidase (GPx), tumor necrosis factor-alpha (TNF α), and interleukin1 beta (IL-1β) genes

The relative abundance of hepatic GPx, TNFα, and, IL-1β messenger ribonucleic acid (mRNA) was determined by qRT-PCR analysis using Glyceraldehyde 3-phosphate dehydrogenase (GAPDH) as a housekeeping gene, as viewed in Table 1 [31]. Nearly, 100 mg of liver tissue was used for total RNA extraction using a total RNA Extraction Kit (Applied Biotechnology, EX02) [32]. After confirming RNA concentration and purity, RT-PCR was carried out using a complementary DNA (cDNA) synthesis kit (Applied Biotechnology, AMP 11) [33]. SYBR green PCR Master Mix (Applied Biotechnology, AMP 03) was used for quantitative assessment of cDNA amplification for each gene [34]. Negative controls, which are template-free, were included [35]. The relative transcription levels were calculated using the comparative $2-\Delta\Delta CT$ method [36].

2.7 Histopathological examination

2.7.1 Light microscopy (L.M.)

Liver samples were carefully dissected from all rats in all groups and fixed in 10% NBF for 48 h. After proper fixation, these samples were washed, dehydrated in ascending grades of ethyl alcohol, cleared in xylene, and embedded in paraffin. They were cut at 3 − 4 µm in thickness for paraffin sections obtained by rotatory microtome, deparaffinized, and stained by hematoxylin & eosin (H&E) according to Bancroft and Gamble [37]. Photomicrographs were captured at different powers to study the histopathological changes using the Leica DM500 microscope and camera (LEICA ICC50 HD).

For the detection of the deviations in the liver tissue, microscopic lesions grading and scoring for hepatic

Table 1 Primer sequence used for qRT-PCR

Gene symbol	Gene description	Accession number	Primer sequence
GAPDH	Glyceraldehyde3-phosphate dehydrogenase	NC_005103.4	F: 5′-ACCACAGTCCATGCCATCAC-3′ R: 5′-TCCACCACCCTGTTGCTGTA-3′
GPX	Glutathione peroxidase	M21210.1	F: 5′-CTCTCCGCGGTGGCACAGT-3′ R: 5-CCACCACCGGGTCGGACATAC-3′
TNFα	Tumor necrosis factor alpha	NM_012675.3	F: 5′-ACACACGAGACGCTGAAGTA-3′ R: 5′-GGAACAGTCTGGGAAGCTCT-3′
IL-1β	Interleukin-1 beta	NM_031512.2	F: 5′- TTGAGTCTGCACAGTTCCCC -3′ R: 5′- GTCCTGGGGAAGGCATTAGG -3′

damage was achieved and evaluated according to Hashim et al. [38]. The hepatic damage was assessed in at least six sections, demonstrating six rats/group for any histopathological deviations. These histopathological lesions were graded and scored on a scale of 0–4 in this fashion: (0) normal histological structure without any deviation, mild (1 < 25%), moderate (2 = 25–50%), severe (3 = 50–75%), and extensive severe tissue damage (4 > 75%).

2.7.2 Immunohistochemical examination

2.7.2.1 Interleukin 1 beta (IL-1β) IL-1β is a potent pro-inflammatory cytokine. Liver sample paraffin sections were dewaxed and hydrated (Merck 1109). Followed by thermal repair to the section antigen, then elimination of endogenous peroxidase activity through incubation for 10 min with 3% H_2O_2 occurs. Next, they were washed with phosphate-buffered saline (PBS) 3 times for 2 min. Later, 30-min incubation at 37 °C with E-IR-R217A (Normal Goat Blocking Buffer) is done. After that, careful shaking was needed to remove the extra fluid. The next step was incubation with the 1ry antibody (Anti-Rabbit IL-1 beta recombinant multiclonal rabbit—antibody [RM1009], Abcam Company, catalog No: ab283818) with a 1:500 dilution and incubation at 20:37 °C for 1 h. After that, they were 3 times washed with PBS 2 min each. It is followed by the dryness of the section using absorbent paper. Later on, incubation with E-IR-R217B (poly peroxidase-anti-mouse IgG) at room temperature for 20 min is done followed by the washing step (PBS for 2 min. 3 times). Fresh 3,3′-diaminobenzidine (DAB) was prepared. The DAB coloring period is controlled until obtaining a tan or brownish yellow. Next, the section is rinsed with deionized water. Following this, the chromogenic reaction is terminated. Subsequently, the counterstaining process is carried out, followed by the steps of dehydration, transparentizing, and sealing. Then incubation with the 2ry antibody (biotinylated mouse anti-rabbit immunoglobulin) for 30 min (the avidin–biotin complex) is done [39].

2.7.2.2 Evaluation of immunohistochemical observations (area percent) for IL-1 β The Leica Quin 500 analyzer computer system is utilized for the analysis of immunohistochemically stained sections. The immunohistochemistry reactions in each group were evaluated by analyzing 5 fields from different slides. The reactions were quantified as a percentage of the total area observed with a magnification power of 400× using light microscopy. Irrespective of the level of staining intensity, the regions demonstrating a positive immunohistochemical response were selected for assessment. The mean value and standard error (SE) were assessed for each sample and subjected to statistical analysis.

2.8 Statistical analysis

The results were expressed as the mean ± SE. For normality, using the Shapiro–Milk test, the parametric data were analyzed by using one-way analysis of variance (ANOVA) to determine the significance of the mean between the groups, followed by a Tukey post hoc test. The nonparametric data of histopathological scoring were analyzed by the Kruskal–Wallis test, followed by the Mann–Whitney *U* test to compare groups according to Noshy et al. [40]. A P value < 0.05 was considered statistically significant. The data were analyzed using SPSS software version 25.

3 Results

3.1 Characterization of CuO-NPs

3.1.1 XRD

From the previously studied XRD pattern of the CuO-NPs, all the previously reported peaks [41] of the as-prepared compound are found in high purity with good intensity. Moreover, the found planes are well matched to Tenorite [JCPD file No. 01-080-1916], which revealed monoclinic CuO crystallites. The value of the crystallite size was calculated using the Scherrer equation based on the main diffraction line (111) and found to be 18 nm. These typical crystal surfaces verify the single-phase nanoscale formation of crystalline CuO particles.

3.1.2 TEM

Figure 1 displays a TEM image of the CuO-NPs produced from the combustion technique and shows some agglomerations as well as many spherical and monoclinic-like structures with moderate sizes ranging from 8 to 20 nm as appeared in the previous study at different power [41].

3.1.3 ZP measurements

Figure 2 shows the obtained results of the ZP and dynamic light scattering (DLS) of the as-prepared CuO-NPs. The surface charge (ZP) is found to be − 23.2 mV, which implies the possible affinity of the CuO-NPs toward the charged biological cells. The size average of about 100% of the dispersed sample in water is 314.5 nm, with a polydispersity index (PDI) of 0.491.

3.1.4 FTIR

The FTIR spectrum of the CuO-NPs synthesized via combustion technique (Fig. 3) shows bands at 3665 (w), 2986 (s), 2884 (s), 1397 (w), 1065 (s), 896 (sh), 652 (sh), 591 (s), and 530 (s) cm − 1.

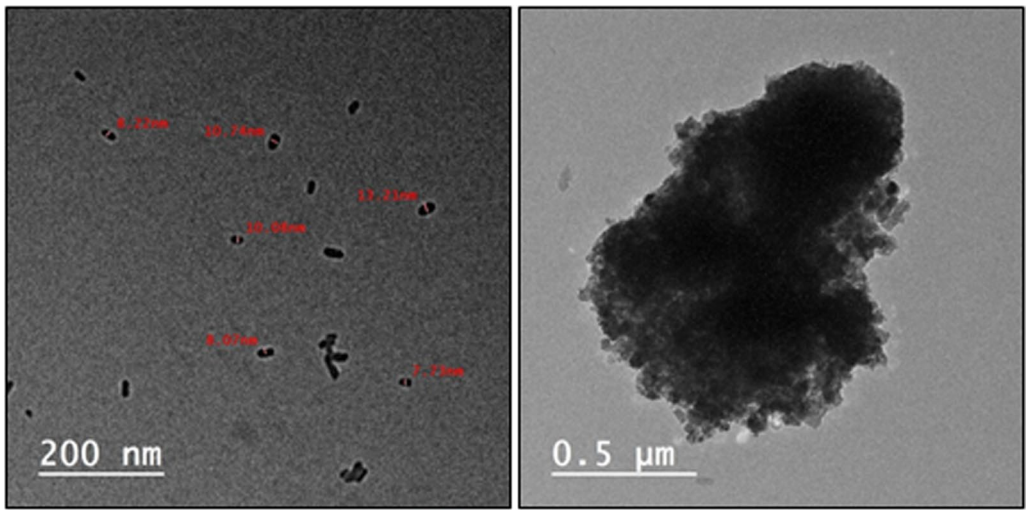

Fig. 1 TEM images of CuO-NPs

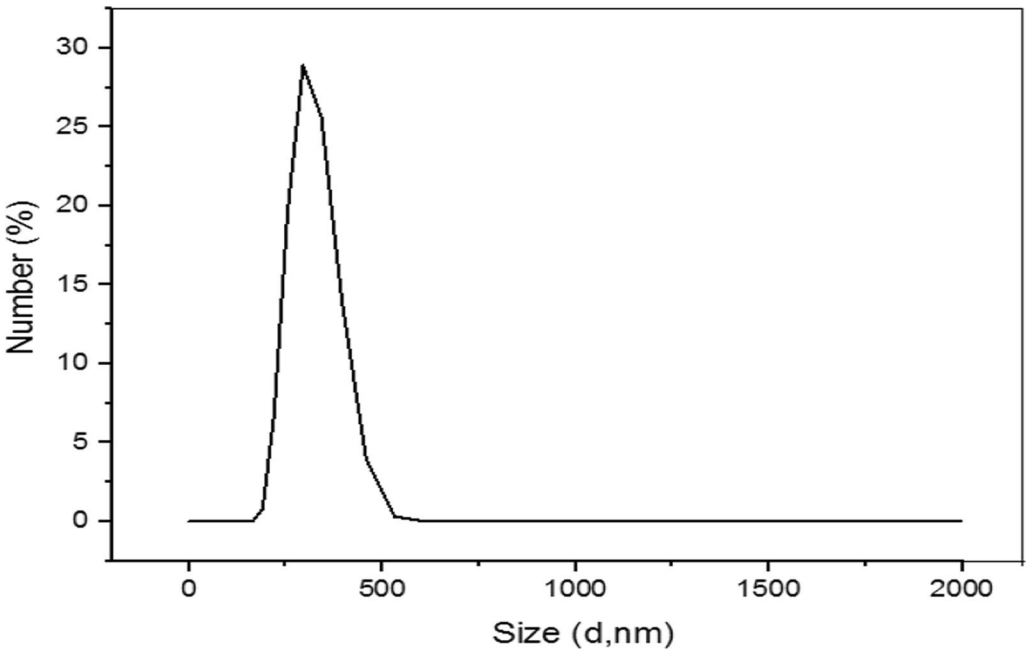

Fig. 2 Particle size distribution by number of the CuO-NPs

3.1.5 Raman

The Raman active modes of CuO-NPs resulted in three peaks around 284, 330, and 623, respectively, as shown in Fig. 4.

3.2 Biochemical analysis

3.2.1 Liver function tests

Figure 5 reveals that CuO-NPs significantly elevated ALT and AST activities when compared with the control group ($p \leq 0.05$). The betaine -co-treated group showed a significant decrease in ALT and AST activities when compared with the CuO-NPs-exposed group ($p \leq 0.05$).

3.2.2 Oxidative stress biomarkers

Oxidative stress biomarkers of liver tissue were determined by the assessment of GSH and MDA levels. CuO-NPs induced oxidative stress in the hepatic tissue, which was indicated by a significant decrease in GSH and an

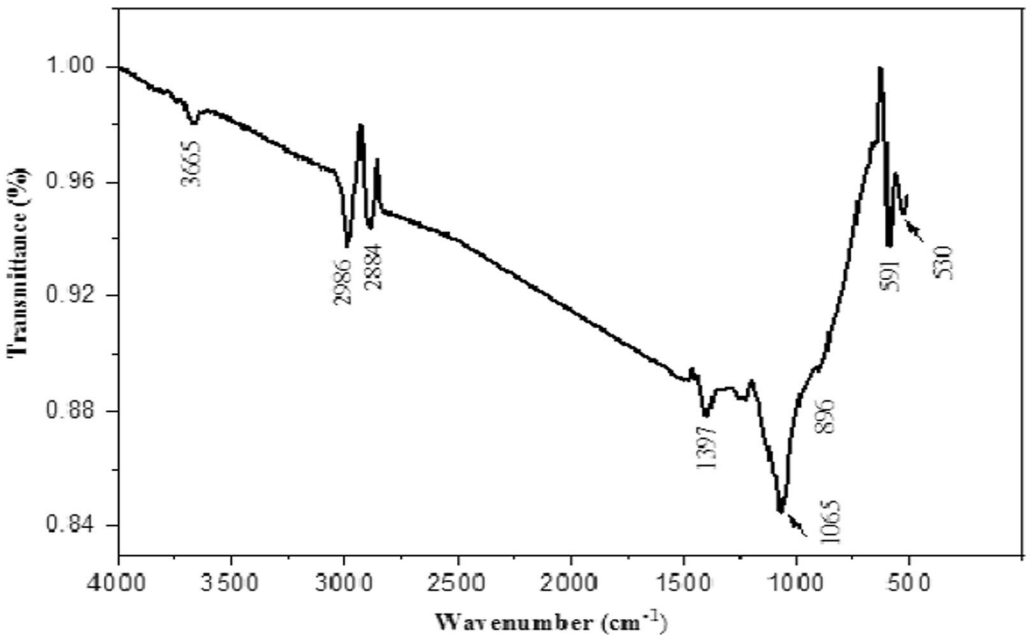

Fig. 3 FTIR spectra of CuO-NPs

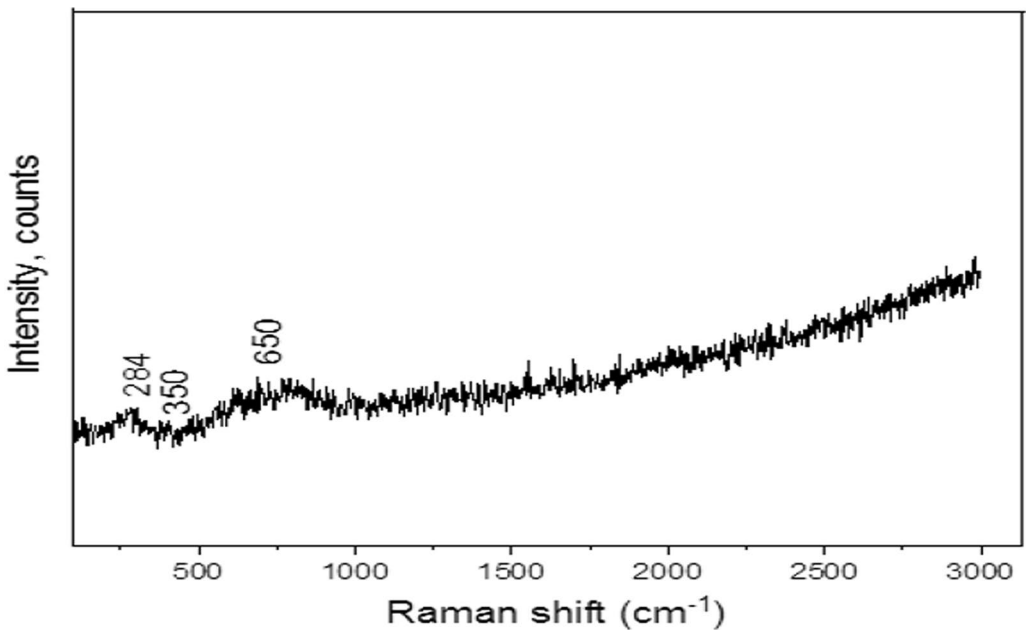

Fig. 4 Raman spectra of the prepared CuO-NPs

increase in MDA in comparison with the control group ($P \leq 0.05$). As shown in Fig. 6, betaine co-treatment ameliorated the oxidative stress induced by CuO-NPs via the significant increase in GSH and decrease in MDA levels in comparison with the CuO-NPs-treated group ($P \leq 0.05$).

3.2.3 qRT-PCR analysis for GPx, TNFα, and IL 1β genes

3.2.3.1 Hepatic mRNA relative expression of GPx gene The GPx gene showed a significant down-regulation in the CuO-NPs-exposed group by 0.18-fold in

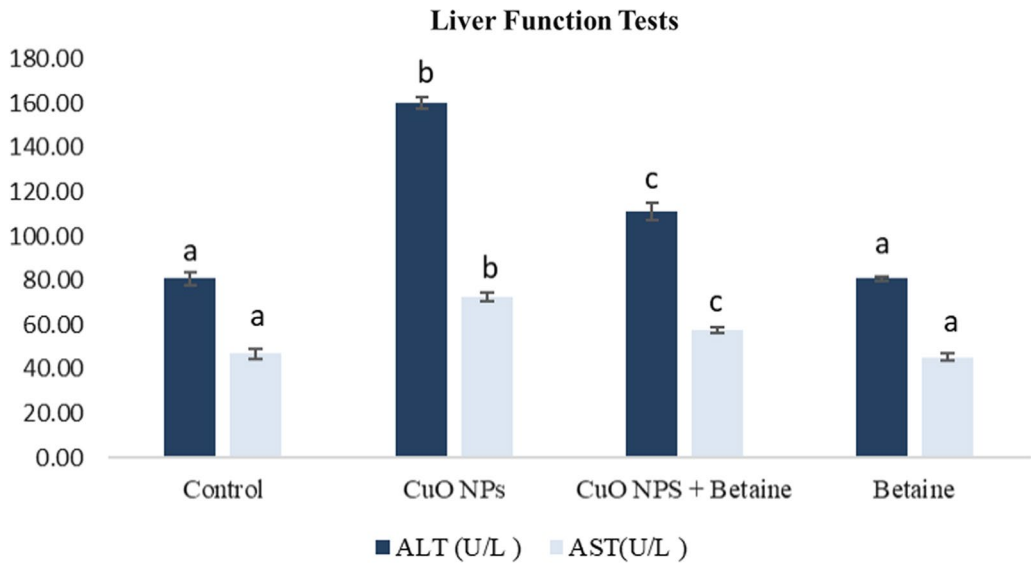

Fig. 5 Effects of CuO-NPs and betaine on ALT and AST activities (U/L) in male albino rats. Data are represented as mean ± SEM. Groups having different letters are significantly different from each other at $P \leq 0.05$. Groups having similar letters are non-significantly different from each other at $P \leq 0.05$

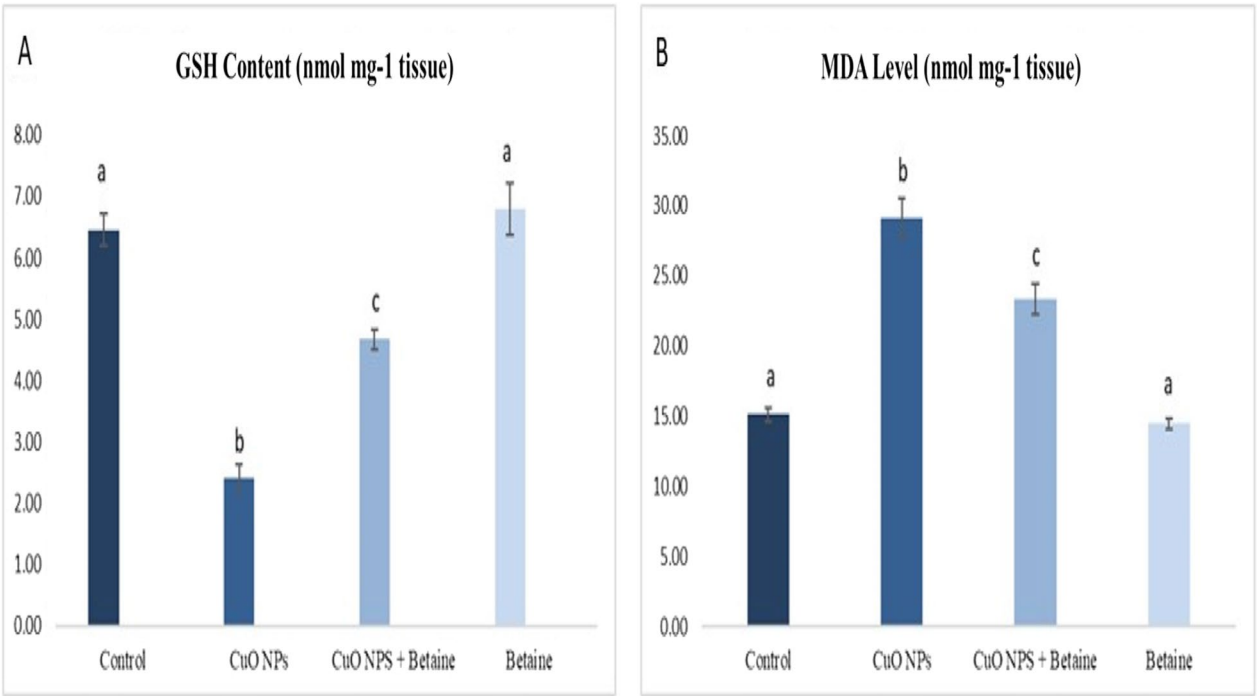

Fig. 6 Effects of CuO-NPs and betaine on the levels of GSH and MDA (nmol mg-1 tissue) in male albino rats. Data are represented as mean ± SEM. Groups having different letters are significantly different from each other at $P \leq 0.05$. Groups having similar letters are non-significantly different from each other at $P \leq 0.05$

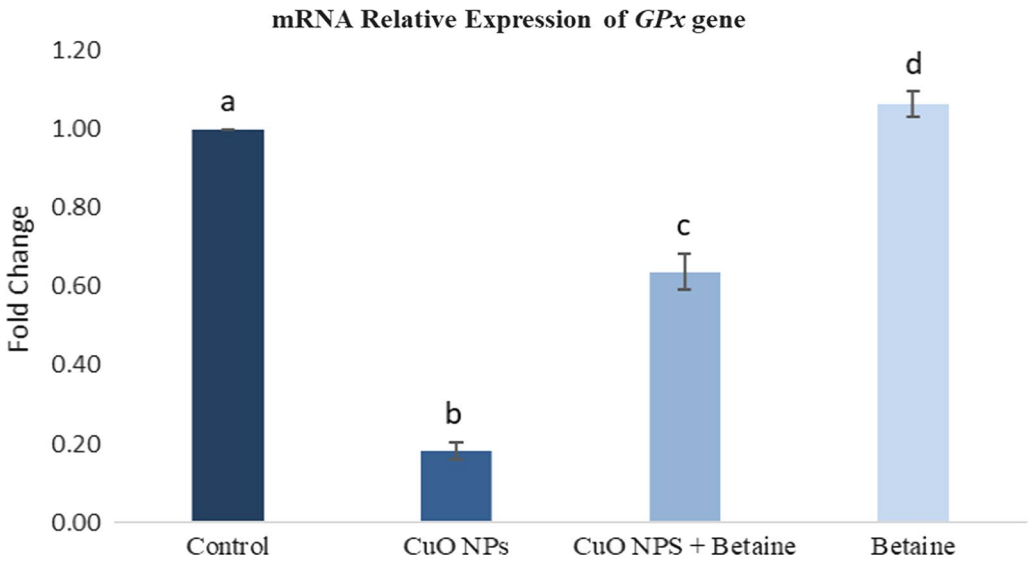

Fig. 7 Effects of CuO-NPs and betaine on hepatic GPx gene expression in male albino rats. Data are represented as mean ± SEM. Groups having different letters are significantly different from each other at $P \leq 0.05$. Groups having similar letters are non-significantly different from each other at $P \leq 0.05$

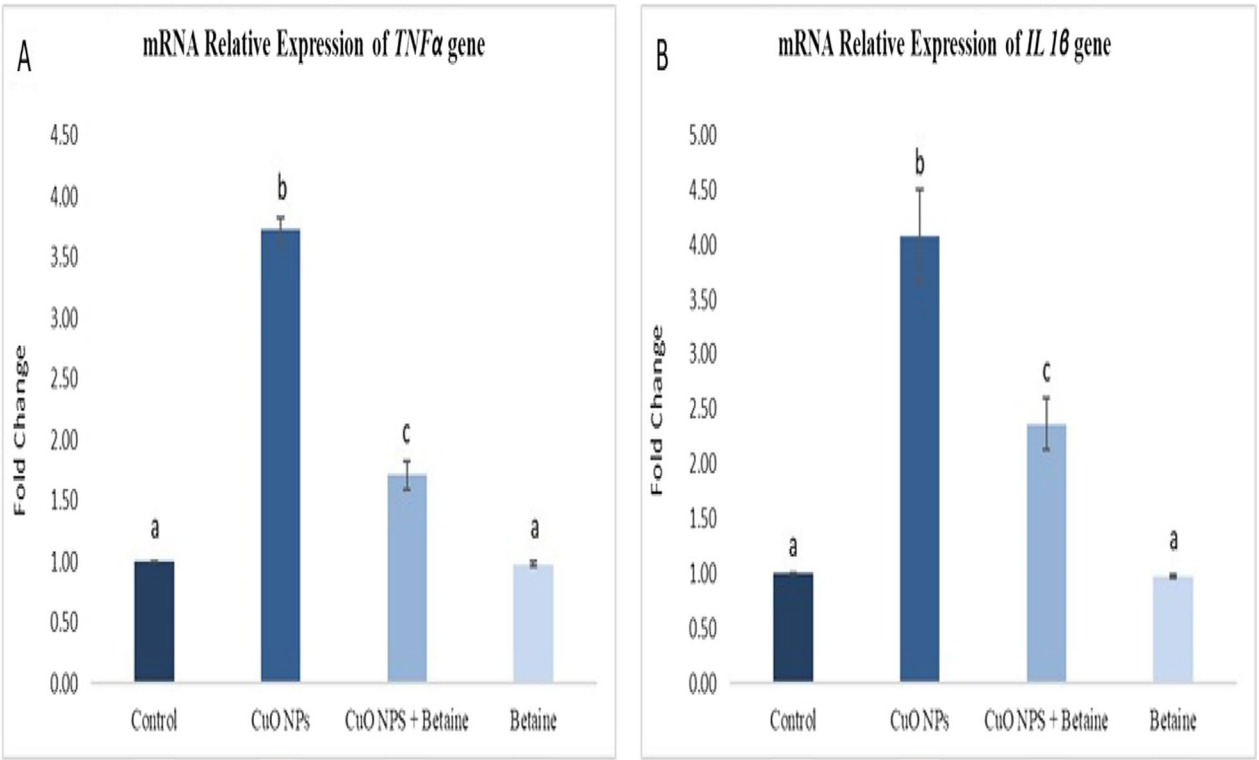

Fig. 8 Effects of CuO-NPs and betaine on mRNA relative expression of some inflammation-related genes (**A**) TNFα (**B**) IL-1β in male Albino rat. Data are represented as mean ± SEM. Groups having different letters are significantly different from each other at $P \leq 0.05$. Groups having similar letters are non-significantly different from each other at $P \leq 0.05$

hepatic tissues compared with the negative control one ($P \leq 0.05$). Betaine co-treatment significantly upregulated the expression level of the GPx gene in comparison with the CuO-NPs group ($p \leq 0.05$) as shown in Fig. 7.

3.2.3.2 mRNA relative expression of some inflammation-related genes (TNFα and IL-1β) According to the data obtained in Fig. 8, CuO-NPs significantly upregulated the liver expression of the TNFα and IL-1β genes by 3.72 and 4.08-fold, respectively, compared with the control group ($P \leq 0.05$). Betaine co-treatment resulted in significantly downregulated hepatic expression of both genes in comparison with the CuO-NPs-treated group ($P \leq 0.05$).

3.3 Histopathological examination

3.3.1 Light microscopic observations

3.3.1.1 Hepatic parenchyma Examination of control rats (group I) liver sections stained with H&E exhibited a normal histoarchitecture of hepatic parenchyma with the presence of normal central veins from which hepatic cords were radiated. These hepatic cords were separated by normal hepatic sinusoids and consisted of hepatocytes, which appeared polygonal in shape with central, spherical, and euchromatic nuclei (Fig. 9A).

In contrast, examination of liver sections of CuO-NPs-exposed rats (group II) demonstrated injurious histopathological deviations in comparison with those of the control group, such as congestion, dilatation, and hyalinization with some vacuolation in the central veins. Hemorrhage beside the central vein was also noticed (Fig. 9B). For the sinusoids, they appeared dilated when compared with those of the control one. Regarding hepatocytes, some of them displayed fatty accumulation (severe micro vesicular steatosis) (Fig. 9C). Others revealed foamy cytoplasmic vacuolation and ballooning (hydropic degeneration). These vacuoles coalesced leading to the complete loss of the acidophilia in some hepatocytes (Fig. 9C, D). Some hepatocytes appeared with pyknotic nuclei and condensed acidophilia, representing necrosis either in individual cells resembling single-cell necrosis (Fig. 9B) or in groups of cells resembling spotty or focal necrosis. The necrotic area was also vacuolated. In addition, there was an increase in the amount of binucleated cells (Fig. 9E). The disorganization of hepatic cords was also noticed (Fig. 9D).

Happily, on examination of liver sections from those co-treated with betaine (group III), there was a partial recovery demonstrated by obvious improvement in the injurious histopathological changes. The hepatic cords appeared regular with a reduction in dilatation and congestion of the central vein with, a complete disappearance of hyalinization and vacuolation. However, the dilatation of sinusoids was also reduced, but some sinusoids were still dilated. Some hepatocytes returned to their normal appearance to a great extent and appeared nearly normal, but others still had pyknotic nuclei (Fig. 9F). Moreover, there was a noticeable decrease in the amount of binucleated cells (Fig. 9G).

Examination of betaine-treated rats (group IV) liver sections showed a normal histoarchitecture of hepatic parenchyma resembling the control group in the presence of a normal central vein, displayed intact endothelium, and radiating from it cords of hepatocytes, which appeared polygonal with central, spherical, and vesicular nuclei. Normal hepatic sinusoids separate these cords (Fig. 9H).

3.3.1.2 Portal triad Examination of control rats (group I) liver sections stained with H&E exhibited a normal histoarchitecture of the portal triads, surrounded by interlobular connective tissue consisting of normal branches of portal veins and hepatic arteries with their intact tunics. Normal bile ducts with their simple cuboidal epithelial lining were also demonstrated (Fig. 10A).

(See figure on next page.)

Fig. 9 Liver section (hepatic parenchyma) of albino rats (H&E ×400) **A** control group (Group I) presenting normal architecture; central vein (CV) displayed intact endothelium, radiating from it cords of hepatocytes, which appeared polygonal with central, spherical and vesicular nuclei (black arrows), and normal blood sinusoids separate these cords (yellow arrows). **B**: **E** CuO-NPs-exposed rats (Group II) revealing **B** dilatation, congestion (yellow star) and hyalinization (H) with vacuolation (black circle) of central vein (CV), hemorrhage (red arrow), and some hepatocytes detected with pyknotic nuclei and more acidophilic cytoplasm (single cell necrosis) (white circles). **C** Severe microvesicular steatosis (black chevrons), and vacuolation of hepatocytes (blue circles) and sinusoidal dilatation (yellow arrows). **D** Hepatic cord disorientation (red star), some hepatocytes exhibited cytoplasmic vacuolation and ballooning (black arrows), and others suffered from complete loss of their acidophilia (red circles). **E** Hepatocytic alterations in the form of focal or spotty necrosis (black stars), vacuolation (black circle), and obvious increase of binucleated cells (green chevrons). **F**–**G** Betaine-co-treated rats (Group III) exhibited partial recovery appeared as: **F** decreased congestion & dilatation of central vein (CV) and sinusoids (yellow arrow) but some sinusoids still dilated (grey arrow), nearly normal hepatocyte (black arrows), and others still suffering from nuclear pyknosis (green arrow). **G** Reduction at binucleation (green chevrons). Notice: regular hepatic cords with nearly normal hepatocytes (black arrow) and sinusoids (yellow arrow). **H** Betaine-treated rats (Group IV) displayed normal central vein (CV), cords of hepatocytes (black arrows), and normal blood sinusoids separate these cords (yellow arrows)

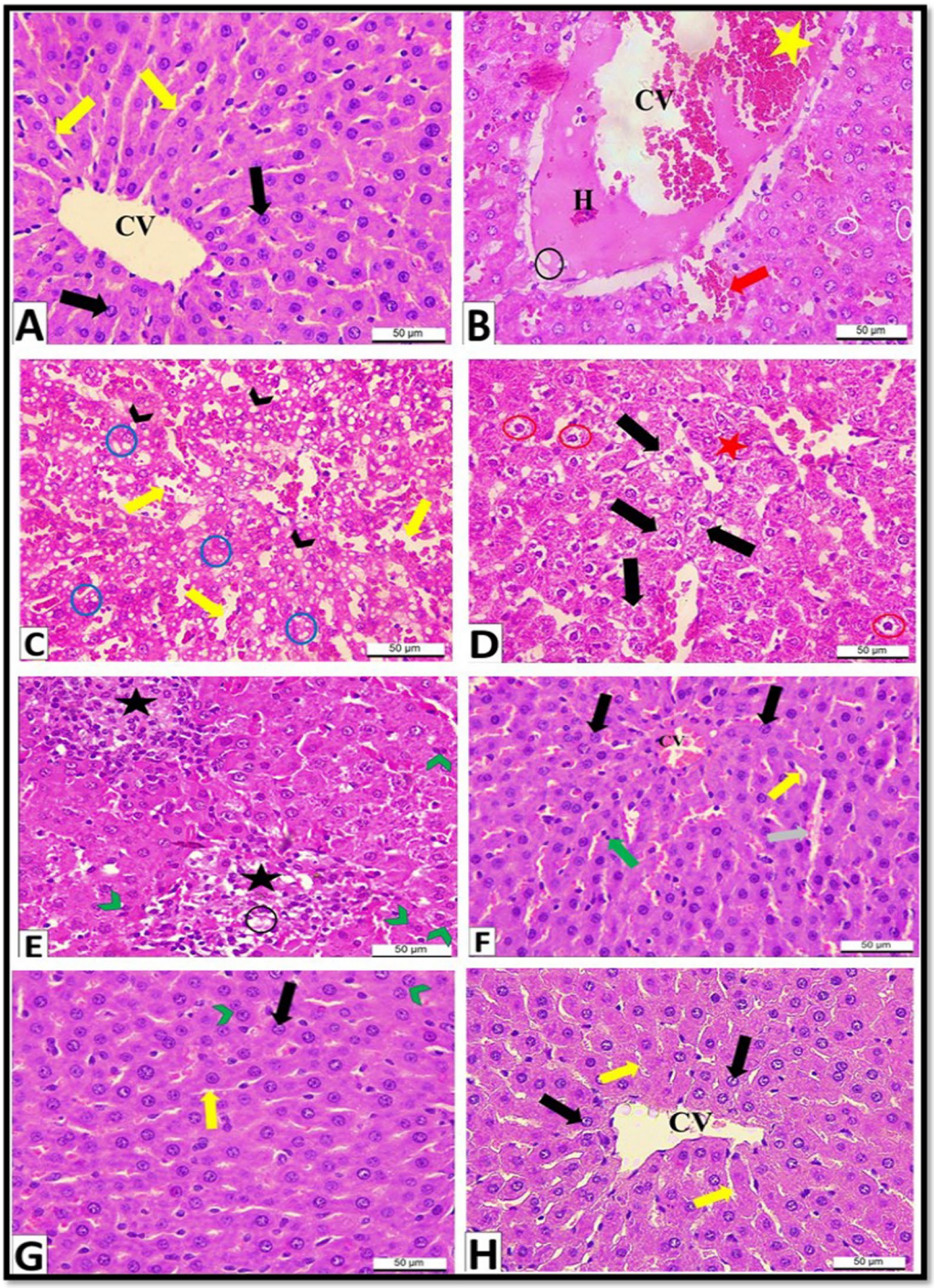

Fig. 9 (See legend on previous page.)

On the other hand, examination of liver sections of CuO-NPs-exposed rats (group II) presented numerous histopathological deviations in the portal triads when compared with those of the control group. These deviations were in the form of severe congestion and dilatation of portal vein branches, as well as dilatation of hepatic artery branches. Hemorrhage and interstitial edema leading to dispersion of the portal area structures were also noticed (Fig. 10B). Moreover, hyalinization and vacuolation appeared in the portal areas (Fig. 10C). With regard to the bile ducts, some of them appeared degenerated with vacuolation of their epithelial lining, and

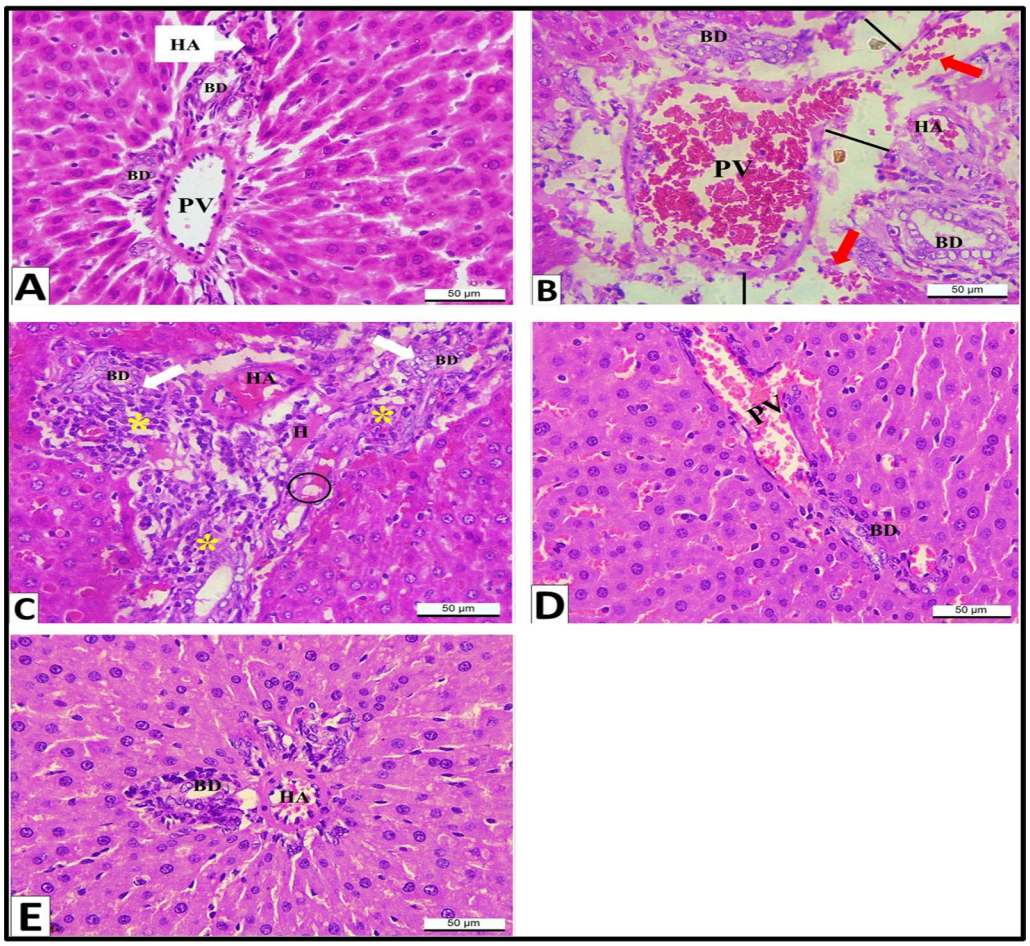

Fig. 10 Liver section (portal triad) of albino rats (H&E ×400); **A** control group (Group I) portal area [bile duct (BD), branch of hepatic artery (HA) (white arrow) and branch of portal vein (PV)]. **B C** CuO-NPs-exposed rats (Group II) revealing: **B** degenerated portal area; severely dilated & congested portal vein branch (PV) and dilated hepatic artery branch (HA), hemorrhage (red arrows), degenerated bile ducts (BD), and edema (black lines). **C** Degenerated bile duct (BD) with epithelial hyperplasia (white arrows), inflammatory cell infiltration (yellow asterisks), and hyalinization (**H**) with vacuolation (black circle) **D** Betaine-co-treated rats (Group III) exhibited partial recovery appeared as bile ducts are nearly normal (BD), decrease at dilatation and congestion of portal vein branch (PV). **E** Betaine-administered rats (Group IV) showing normal portal area [bile duct (BD), hepatic artery (HA)]

others appeared with epithelial hyperplasia (Fig. 10B, C). Inflammatory cell infiltration at portal areas was a characteristic feature of CuO-NPs intoxication (Fig. 10C).

Fortunately, the co-treatment with betaine in group III could alleviate the deleterious changes in the portal triad through a reduction in dilation and congestion of its vessels in comparison with group II and the complete absence of hyalinization. Regarding the bile ducts, there was a marked improvement (Fig. 10D).

Finally, examination of liver sections of betaine-treated rats (group IV) (Fig. 10E) resembled those from the control group and presented a normal histoarchitecture of the portal triads.

For confirmation of the hepatoprotective effect of betaine against CuO-NPs intoxication at the histoarchitecture level, histopathological scoring was obtained. This scoring revealed a significant variance ($p < 0.05$) between different groups by analysis of those co-treated with betaine; there was a significant reduction ($p < 0.05$) when compared to those intoxicated with CuO-NPs, as shown in Tables 2 and 3 in the hepatic parenchyma and portal triad, respectively.

3.3.2 IL-1β Immunohistochemical analysis

Liver sections investigation against IL-1β immunoreactivity revealed a negative immunoreaction in those that belonged to the control rats (Group I) (Fig. 11A). On the other side, there was an intense positive immunoreaction in those CuO-NPs-intoxicated rats (Group II) (Fig. 11B).

Table 2 Microscopic lesions histopathological scoring in different groups of rats at liver (hepatic parenchyma)

	Control rats	CuO-NPs-exposed rats	Betaine-co-treated rats	Betaine-administered rats	*P* value	*F* value
Congestion and dilatation of vessels	0 ± 0^{a}	4 ± 0^{b}	$1.5 \pm 1^{a,b}$	0 ± 0^{a}	0.000	285.000
Hemorrhage	0 ± 0^{a}	3 ± 1^{b}	$1 \pm 0^{a,b}$	0 ± 0^{a}	0.000	222.500
Hyalinization	0 ± 0^{a}	4 ± 1^{b}	$0.5 \pm 1^{a,b}$	0 ± 0^{a}	0.000	132.059
Steatosis	0 ± 0^{a}	4 ± 0.25^{b}	$1 \pm 0.5^{a,b}$	0 ± 0^{a}	0.000	139.118
Degeneration	0 ± 0^{a}	3.5 ± 1^{b}	$1.5 \pm 1^{a,b}$	0 ± 0^{a}	0.000	110.000
Necrosis	0 ± 0^{a}	3.5 ± 1^{b}	$1 \pm 1^{a,b}$	0 ± 0^{a}	0.000	115.588
Binucleation	1 ± 0^{a}	4 ± 0^{b}	$3 \pm 1^{a,b}$	1 ± 0^{a}	0.000	190.000

Results are determined as median ± interquartile range for six rats for the same group

[a] $p < 0.05$ in relation to the CuO-NPs group

[b] $p < 0.05$ in relation to the control group

Table 3 Microscopic lesions histopathological scoring in different groups of rats at liver (portal triad)

	Control rats	CuO-NPs-exposed rats	Betaine-co-treated rats	Betaine-administered rats	*P* value	*F* value
Congestion and dilatation of vessels	0 ± 0^{a}	4 ± 0^{b}	$1.5 \pm 1^{a,b}$	0 ± 0^{a}	0.000	285.000
Hemorrhage	0 ± 0^{a}	3 ± 1^{b}	$1 \pm 0^{a,b}$	0 ± 0^{a}	0.000	222.500
Hyalinization	0 ± 0^{a}	4 ± 1^{b}	$0.5 \pm 1^{a,b}$	0 ± 0^{a}	0.000	132.059
Bile duct degeneration	0 ± 0^{a}	4 ± 0.25^{b}	$1 \pm 0.5^{a,b}$	0 ± 0^{a}	0.000	139.118
Edema	0 ± 0^{a}	3.5 ± 1^{b}	$1.5 \pm 1^{a,b}$	0 ± 0^{a}	0.000	110.000
Inflammatory cells infiltration	0 ± 0^{a}	3.5 ± 1^{b}	$1.5 \pm 1^{a,b}$	0 ± 0^{a}	0.000	115.588

Results are determined as median ± interquartile range for six rats for the same group

[a] $p < 0.05$ in relation to the CuO-NPs group

[b] $p < 0.05$ in relation to the control group

By examination of betaine-co-treated rats (Group III), there was a great decrease in immunoexpression against IL-1β (Fig. 11C). Sections from betaine-treated rats (Group IV) showed negative immunoreactivity against IL-1β as the control one (Fig. 11D).

IL-1β expression quantification proved that CuO-NPs indicated high expression with a significant difference from ($P < 0.05$) other groups. Moreover, betaine-co-treated rats (group III) decreased with a significant difference from all other groups ($P < 0.05$) (Table 4).

4 Discussion

CuO-NPs are extensively used in different life domains as a result of their exclusive physiochemical and biological properties [16]. The tinny size of CuO-NPs facilitates their ability to penetrate and accumulate into different body tissues and organs, including the liver, disrupting their habitual structure as well as affecting the organs' normal function [42].

Betaine is a glycine derivative that has been extensively used for its protective effects against several hepatic diseases, such as alcoholism, fatty liver, and cirrhosis [43].

As the liver represents the principal detoxifying and metabolic organ of the body, about 10% of the population around the world suffers from liver diseases [44]. In addition, it is recognized as a crucial organ that plays a significant role in capturing and eliminating nanoparticles, aided by its reticuloendothelial system [45]. Regardless of the wide use of betaine as a hepatoprotective agent, its exact cytoprotection mechanism remained questionable, and there is a scarcity in its use to counteract the CuO-NPs hepatotoxicity. The current study shed light on assessing the capability of betaine to diminish the hepatotoxicity resulting after intraperitoneal injection of CuO-NPs.

Copper (II) nitrate trihydrate was used in the preparation as a water-soluble copper source, and it acts as a strong oxidizing agent. Fresh egg white was used as a particle size control agent at various calcination temperatures because of its accessibility and suitable price [46]. The egg white is a biological liquid that has great levels of amino acids and proteins, such as albumin and lysosomes [47, 48]. These amino acids have a structure that can act as a stabilizer in the production of nanoparticles [49]. In

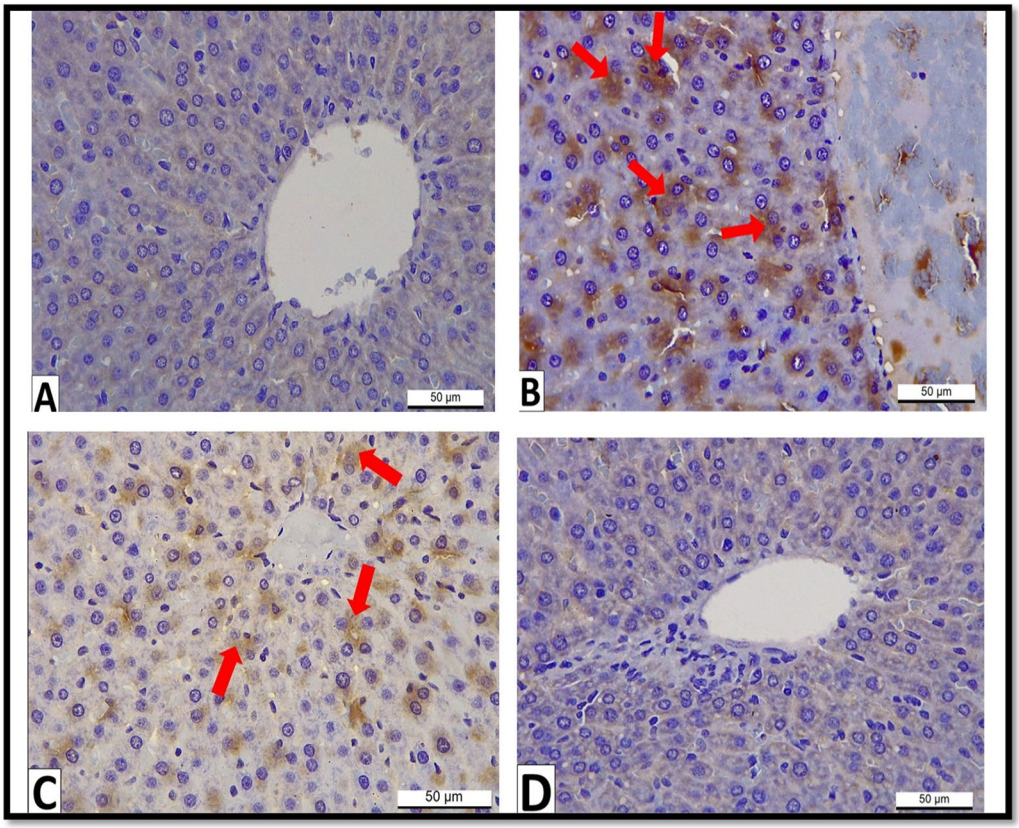

Fig. 11 Immunohistochemically examined liver sections against IL-1β immunoreactivity (×400) **A** control rats (Group I) revealed negligible reaction. **B** CUO-NPs intoxicated rats (Group II) revealed intense positive reaction (arrows). **C** Betaine-co-treated rats (Group III) revealed moderate reaction (arrows). D Betaine-treated rats (Group IV) exhibited negligible reaction

Table 4 IL-1β area (%) in liver sections of different groups

	Control rats	CuO-NPs-exposed rats	Betaine-co-treated rats	Betaine-administered rats	*P* value	*F* value
IL-1β area% (mean ± (SE))	$0.02 \pm 0.016^{b,c}$	$22.55 \pm 0.6^{a,c,d}$	$8.3 \pm 0.3^{a,b,d}$	$0.02 \pm 0.007^{b,c}$	0.000	875.951

Results are presented as means ± standard error (SE), $n = 3$ rats/group. Different superscript letters in the same row indicate significant differences as [a]signifies control negative group (Gp I), [b]signifies CuO-NPs-exposed rats (GP II), [c]signifies betaine-co-treated rats (Gp III), and [d]signifies betaine-administered rats (Gp IV), $p < 0.05$

related research around the world, attempts are made to use industrial and natural amino acids that are commonly costly [50].

The ZP gives important information about the surface charge of the CuO-NPs and their potential electrostatic attraction to biological targets, subsequently affecting their toxicity and activity. The surface charge (ZP) was found to be − 23.2 mV, which implies the possible affinity of the CuO-NPs toward the charged biological cells, therefore affecting their efficacy [51]. The size average of about 100% of the dispersed sample in water is 314.5 nm, with a polydispersity index (PDI) of 0.491. The PDI value indicates the polydisperse particle size distributions and the formation of CuO-NPs. The functionalized CuO-NPs with a negative surface charge might exhibit electrostatic repulsion between cell membranes and nanoparticles [52].

The FTIR spectrum of CuO-NPs synthesized via combustion technique showed bands at 3665 (w), 2986 (s), 2884 (s), 1397 (w), 1065 (s), 896 (sh), 652 (sh), 591(s), and 530 (s)cm^{-1}. The weak band around 3665 cm^{-1} is due to the vibration mode of the absorbed water, while the bending mode exhibited a peak around 1400 cm^{-1} [53]. Two strong bands around 2986 and 2884 cm^{-1} can be seen, and they are attributed to symmetric and asymmetric stretching vibrations of the C-H bond of the organic matter [54]. Moreover, the appearance of bands in the range 400–600 cm^{-1} which are related to the

metal–oxygen (Cu–O) bond, confirmed the formation of CuO-NPs from combustion synthesis [55]. The Cu–O–H bonds led to a bending absorption band around 900 cm^{-1}, while the band at 1065 cm^{-1} is attributed to the C–O stretching vibration [56].

There are nine zone-center optical phonon modes with symmetries 4Au + 5Bu + Ag + 2Bg; which represent the Raman spectrum of the prepared CuO-NPs. As calculated previously, only three Ag + 2Bg from the nine zone-center optical phonon modes are Raman active [57]. These Raman active modes of CuO-NPs resulted in three peaks around 284, 330, and 623, respectively, those are close to the reported wavenumbers in the literature [58, 59].

The accumulation of NPs in various tissues of live creatures might lead to a dose-dependent elevation of cellular ROS [60]. There is increasing evidence suggesting that oxidative stress and inflammation are significant factors in the development of toxicity caused by NPs [40]. Therefore, we conducted an experimental study using adult rats to examine and compare changes in liver tissue after exposure to CuO-NPs. Our study also aimed to investigate the protective effects of betaine, a potent antioxidant, by analyzing oxidant and antioxidant biomarkers as well as pro-inflammatory cytokines.

The current study found that administering CuO-NPs to rats led to the emergence of liver dysfunction, oxidative stress, and inflammation. The study demonstrated a notable increase in the liver function enzymes ALT and AST, as well as in the concentration of MDA, a biomarker for lipid peroxidation. Additionally, there was an elevation in the levels of the pro-inflammatory cytokines IL-1β and TNF-α. Conversely, there was a significant decrease in the concentration of total GSH and the expression level of the GPx enzyme.

Once liver cells are harmed, ALT and AST enzymes are released immediately into the bloodstream, serving as the primary indicators of liver malfunction. In typical circumstances, these enzymes are present in significant amounts in the hepatocytic cytoplasm. However, with liver damage, they are released into the bloodstream, as previously mentioned by Contreras-Zentella and Hernández-Muñoz [61].This is exactly what our results indicate, which is in accordance with Tang et al. [62], Abdel-Azeem et al. [63], Sutunkova et al. [64].

The induction of oxidative stress is widely recognized as a primary mechanism behind the toxicity of nanoparticles [36]. Multiple studies have reported that excessive production of reactive oxygen species (ROS) caused by CuO-NPs disrupts the equilibrium between the liver's oxidative and antioxidant mechanisms. This disruption leads to lipid peroxidation through the generation of ROS and MDA, which is strongly associated with the decline in antioxidant enzymes, as indicated by the present study.

Nano-copper has the ability to penetrate many biological barriers and enter the bloodstream, where it may accumulate in the liver and interact with large biological molecules, resulting in oxidative damage [65]. The primary factor leading to organ damage induced by Cu-NPs is oxidative stress [62]. ROS, in turn, act as mediators to activate the immune system [66]. Inflammation is an additional way in which CuO-NPs cause toxicity. Cells can counteract the excessive oxidative stress response by upregulating the production of cytokines like TNF-α [67]. Interleukin (IL-1) cytokines family are expressed as central inflammatory mediators. Particularly, IL-1β has a vital role in the defense response to damages and injuries [68]. The results of this research were in line with Tang et al. [62], Abdel-Azeem et al. [63]. Moreover, the inflammatory effect of CuO-NPs was confirmed immunohistochemically by enhancing the immunoreactivity toward IL-1β in liver sections of rats exposed to CuO-NPs toxicity (GP II). The same result was conducted earlier by Dumoulin et al. [69] who analyzed IL-1β in the liver of patients with chronic hepatitis C. This over-expression resulted from the ability of CuO-NPs to enhance the inflammatory process via proinflammatory mediators released as IL-1β and TNFα [70].

The presence of CuO-NPs will exacerbate liver dysfunction by inducing oxidative stress and triggering an inflammatory response. Due to their minimal adverse effects and significant safety profile, natural products have emerged as a prominent area of research for human health concerns.

Interestingly, the findings demonstrated that betaine administration markedly decreased the blood concentrations of liver function enzymes, as well as the hepatic tissue levels of MDA. Concurrently, the levels of GSH and GPx exhibited a notable increase. Furthermore, betaine can significantly mitigate liver impairment generated by CuO-NPs by a mechanism that involves the decrease of the pro-inflammatory cytokines IL-1β and TNFα. Several prior studies have demonstrated the hepatoprotective properties of betaine against various forms of liver damage [71].

The observed activation of the antioxidant system may be attributed to the upregulation of genes responsible for antioxidant defense. Tang et al. [62] also reported comparable findings. Betaine has the ability to augment the antioxidant activity of liver cells, stimulate the growth and renewal of liver cells, and preserve or safeguard the functioning of mitochondria and Golgi apparatus. Prior studies hypothesized that betaine's antioxidant activities were attributed to its capacity to eliminate free radicals [72].

The efficacy of betaine in combating oxidative stress is contingent upon its lipotropic properties, which facilitate its easy passage through the lipid bilayer membrane and diffusion into the intracellular compartment [73]. Betaine functions as a provider of methyl groups for the conversion of homocysteine to methionine in a metabolic process facilitated by betaine-homocysteine methyltransferase (BHMT). Studies have demonstrated that administering betaine to rats increases the levels of hepatic methionine and S-adenosylmethionine via inducing BHMT [74]. GSH is a crucial chemical that is created based on this pathway and serves as a notable endogenous antioxidant. The anti-inflammatory properties of betaine have been extensively documented in multiple investigations, including those by Zhai et al. [71], Arumugam et al. [72]. The immunohistochemical analysis verified the anti-inflammatory impact of betaine by demonstrating a significant reduction in the intensity of IL-1β immunoexpression in liver sections of rats co-treated with betaine (group III). Thus, betaine may have the potential to decrease the production of C-reactive protein, IL-6, and TNFα activities, as well as suppress the pro-inflammatory production and release of IL-1β [75]. The key factor contributing to betaine's anti-inflammatory activity is the increase in the antioxidant defense system [72]. Betaine, a potent antioxidant, mitigated the production of inflammatory mediators and enhanced tissue regeneration by diminishing degenerative alterations [76].

The results of the current study verified several histopathological deviations in the hepatic tissue of rats subjected to CuO-NPs (GP II) in comparison with those of the control group (GPI) and those administered with betaine (GPVI). These deviations included severe congestion, dilatation, and hyalinization of the central veins and portal vein branches, as well as dilatation of the hepatic artery's branches and sinusoids, plus hemorrhage. These findings came in agreement with Arafa et al. [3], Ghonimi et al. [77]. Arafa et al. injected rats intraperitoneally with 3 and 50 mg/kg for 7 successive days, and Ghonimi et al. subjected rats to a daily dose of CuO-NPs of 5, 10, and 25 mg/kg intraperitoneally for 9 days. These vascular changes might be attributed to mononuclear cell infiltration [78]. In addition, the ability of Cu-NPs to elevate the production level of vasodilators as prostaglandin E2 (PGE2) and enhance the inflammatory process via proinflammatory mediator release as IL-1β and TNF α [70]. As well as, the authors of the current study hypothesize that the severe vascular congestion of the central and portal veins may cause mechanical pressure on their wall, leading to its impairment and rupture, causing blood extravasation (hemorrhage).

The hepatocytic alterations observed in this study, such as fatty accumulation (severe steatosis) and hydropic degeneration, ranged from cytoplasmic vacuolations and ballooning of the cell to complete loss of cellular acidophilia. These observations were in parallelism with Ghonimi et al. [77], Tohamy et al. [79]. Tohamy et al. orally gave rats at a dose of 100 mg/kg for 14 consecutive days. CuO-NPs also led to hepatocellular necrosis, which ranged from single-cell necrosis to a group of cells or focal area of the liver (focal or spotty necrosis). De Jong et al. [19], Tohamy et al. [79] also confirmed the necrotic lesions caused by CuO-NPs. De Jong et al. treated rats orally with 0.1 mg/20 g for 5 successive days. Cheville [80] hypothesized hepatocytic alterations, as they are the main site for toxicity due to their lower content of oxygen and having several toxin receptors on their surfaces. Also, these observed hepatocytic deviations may be a result of the release of Cu which is a water-soluble ion, as mentioned by Elhussainy and El-Shourbagy [81]. The cellular swelling might be attributed to the disturbance of the ion pump of the plasma membrane, which disturbs the fluid homeostasis, which in turn results in the entrance of fluid inside the cell [82]. Besides, hepatocytic ballooning and vacuolation may be a type of defense mechanism versus any harmful substances [83]. The occurrence of lipid droplets signifies a reduction in cytoplasmic protein synthesis, so triglycerides transport for prevention of lipoprotein formation [80]. Loss of cellular acidophilia may be attributed to loss of cellular organelles [38]. Cho et al. [84] assumed that CuO-NPs diminish the viability of the cell via DNA binding, leading to DNA damage and consequently cell death. Cho et al. [84] added that the cell toxicity is due to the marked elevation of IL-1β, IL-8, and TNF-α. Furthermore, oxidative stress and excessive lipid peroxidation cause mitochondrial failure and, finally cell death [85]. Also, Tohamy et al. [79] postulated that hepatocytic necrosis is due to a reduction in protein synthesis. The current study also demonstrated an abnormal increase in the binucleated cells, which regards a type of detoxification response of the liver and a modification of the activity of the cell cycle [86]. The disorientation of hepatic cords could be a result of these hepatocytic deviations that caused failure of cellular contact with neighboring cells.

This investigation also demonstrated histopathological alterations in the portal triads, such as degenerated bile ducts, hyperplasia of the duct epithelial lining, and infiltration with mononuclear inflammatory cells. Abdelazeim et al. [27], Tohamy et al. [79] also noted these results. As CuO toxicokinetics revealed, the overloaded Cu^{+2} ions in circulation are eliminated via the liver through the bile duct in the bile and absorbed through the intestine, partially later on pumped again

via the portal vein back to the liver [87]. This may initiate portal area deviations as a self-defense mechanism, which regards ductular reaction as an essential factor for hepatic regeneration during damage to both hepatocytes and cholangiocytes [88].

Interestingly, the light microscopical investigations for liver sections from those co-treated with betaine (GP III) in comparison with those of group II displayed partial recovery in the form of reduction of dilation and congestion of affected blood vessels and complete disappearance of hyalinization and vacuolation. Some hepatocytes are nearly normal with central, spherical, and vesicular nuclei while others still have pyknotic nuclei. Concerning portal triads, there was a great reduction in their histopathological changes and they appeared nearly normal. These observations were concomitant with those of Abdel-Daim and Abdellatief [30], Heidari et al. [43]. Abdel-Daim and Abdellatief administered betaine to alleviate abamectin toxicity by 250 mg/kg daily for 10 days orally, and Heidari et al. concluded that betaine administration at doses of 10 and 50 mg/kg could lessen alterations in the hepatic tissue of cirrhotic animals. These improvements in hepatic tissue are due to the powerful antioxidant capacity of betaine [89]. Besides its ability to maintain the structural integrity and normal functions of plasma membranes [89]. Betaine can maintain membranes' normal status via its assistance in the methylation of cell membranes and, consequently sustain phosphatidylcholine-phosphatidylethanolamine balance [90]. Betaine also promotes the oxidation process of fatty acids and improves lipid metabolism, as well as increasing high-density lipoprotein cholesterol (HDL-c) level, which interprets the reduction of hepatic steatosis [91]. The reduction of inflammatory cell infiltration is due to betaine obstructing the nuclear factor-κB (NF-κB) signaling pathway, which controls several genes involved in inflammation, such as TNFα, IL-1β, and IL-23 [22].

5 Conclusion

Based on this investigation, we have shown that CuO-NPs have the potential to disrupt the normal functioning of the liver through biochemical, histopathological, and immunohistochemical changes. Additionally, betaine has been found to be effective in reducing these changes. Hence, we suggest administering betaine as a safeguarding agent to individuals who are anticipated to be more susceptible to CuO-NPs exposure, particularly those residing in industrial regions. Despite the administration of betaine, mild degenerative changes are still present in the hepatic tissue. Therefore, additional research is necessary to discover the optimal dosage for maximum improvement, particularly since this is the first study to utilize betaine as a protective agent against hepatotoxicity caused by CuO-NPs.

Abbreviations

NPs	Nanoparticles
Cu-NPs	Copper nanoparticles
CuO-NPs	Copper oxide nanoparticles
ALT	Alanine aminotransferase
AST	Aspartate aminotransferase
MDA	Malondialdehyde
GSH	Glutathione
GPX	Glutathione peroxidase
GSSG	Oxidized glutathione
IL-1β	Interleukin1 beta
IL-6	Interleukin-6
TNF-α	Tumor necrosis factor alpha
MRSA	Methicillin-resistant *Staphylococcus aureus*
E. coli	*Escherichia coli*
RS	Reactive species
ROS	Reactive oxygen species
DNA	Deoxyribonucleic acid
cDNA	Complementary deoxyribonucleic acid
CYP450	Cytochrome P 450
ALP	Alkaline phosphatase
SAM	S-adenosylmethionine
CCl4	Carbon tetra chloride
FTIR	Fourier-transform infrared
XRD	X-ray diffraction
DLS	Dynamic light scattering
PDI	Polydispersity index
min	Minutes
g	Gram
IACUC	Institutional Animal Care and Use Committee
n	Number
mg/kg	Milligram per kilogram
rpm	Repeat per minute
qRT-PCR	Quantitative real time polymerase chain reaction
NBF	Neutral-buffered formalin
GAPDH	Glyceraldehyde 3-phosphate dehydrogenase
RNA	Ribonucleic acid
mRNA	Messenger ribonucleic acid
L.M	Light microscopy
h	Hour
μm	Micrometer
H&E	Hematoxylin & eosin
PBS	Phosphate buffer saline
DAB	Diaminobenzidine
SE	Standard error
ANOVA	Analysis of variance
BHMT	Betaine-homocysteine methyltransferase
GP	Group
HDL-c	High-density lipoprotein cholesterol
NF-κB	Nuclear factor-κB

Acknowledgements

Not applied for this manuscript.

Author contributions

Prof. El-G.S.M. conceived the study and designed the experimental protocol. A.R.H., D.W.B., E.R. carried out the histopathological analysis and draft the manuscript. N.M.D., E.A.D.h prepared and made the nanoparticles characterization. Mona K. Galal, Maha M. Rashad carried out the biochemical analysis. All authors read, revised, and approved the final manuscript.

Funding

This research did not receive any specific grant from funding agencies in the public, commercial, or not for profit sectors.

Availability of data and materials

Not applicable.

Declarations

Ethics approval and consent to participate
All animals were humanely cared in accordance with the protocol accepted by the Institutional Animal Care and Use Committee (IACUC) of the Faculty of Veterinary Medicine, Cairo University (protocol no. Vet CU03162023754).

Consent for publication
Not applicable.

Competing interests
The authors have no conflict of interest to declare.

Author details
[1]Cytology and Histology Department, Faculty of Veterinary Medicine, Cairo University, Giza, Egypt. [2]Biochemistry and Chemistry of Nutrition Department, Faculty of Veterinary Medicine, Cairo University, Giza, Egypt. [3]Physical Chemistry Department, National Research Centre, Dokki, Giza, Egypt. [4]Inorganic Chemistry Department, National Research Centre, Dokki, Giza, Egypt.

Received: 19 January 2024 Accepted: 13 May 2024
Published online: 20 May 2024

References

1. Naz S, Gul A, Zia M (2020) Toxicity of copper oxide nanoparticles: a review study. IET Nanobiotechnol 14(1):1–13
2. Jahanbakhshi A, Hedayati A, Pirbeigi A (2015) Determination of acute toxicity and the effects of sub-acute concentrations of CuO nanoparticles on blood parameters in Rutilus rutilus. Nanomed J 2(3):203–213
3. Arafa AF, Ghanem HZ, Soliman MS, Emad EM (2017) Modulation effects of quercetin against copper oxide nanoparticles-induced liver toxicity in rats. Egypt Pharm J 16(2):78–86
4. Uclés A, López SH, Hernando MD, Rosal R, Ferrer C, Fernández-Alba AR (2015) Application of zirconium dioxide nanoparticle sorbent for the clean-up step in post-harvest pesticide residue analysis. Talanta 144:51–61
5. Aksakal FI, Ciltas A (2019) Impact of copper oxide nanoparticles (CuO NPs) exposure on embryo development and expression of genes related to the innate immune system of zebrafish (*Danio rerio*). Comp Biochem Physiol C Toxicol Appl Pharmacol 223:78–87
6. Sicwetsha S, Mvango S, Nyokong T, Mashazi P (2021) Effective ROS generation and morphological effect of copper oxide nanoparticles as catalysts. J Nanopart Res 23:1–18
7. Alexandru C, Dragoi B, Ungureanu A, Ciotonea C, Mazilu I, Royer S, Mamede A-S, Rombi E, Ferino I, Dumitriu E (2016) Facile synthesis of highly dispersed and thermally stable copper-based nanoparticles supported on SBA-15 occluded with P123 surfactant for catalytic applications. J Catal 339:270–283
8. Assadian E, Zarei M, Ghanadzadeh Gilani A, Farshin M, Dezhampanah H, Pourahmad J (2018) Toxicity of copper oxide (CuO) nanoparticles on human blood lymphocytes. Biol Trace Elem Res 184:66
9. El Bialy BE, Hamouda RA, Abd Eldaim MA, El Ballal SS, Heikal HS, Khalifa HK, Hozzein WN (2020) Comparative toxicological effects of biologically and chemically synthesized copper oxide nanoparticles on mice. Int J Nanomed 15:3827–3842
10. Elkhateeb SA, Ibrahim TR, El-Shal AS, Abdel Hamid OI (2020) Ameliorative role of curcumin on copper oxide nanoparticles-mediated renal toxicity in rats: an investigation of molecular mechanisms. J Biochem Mol Toxicol 34(12):e22593
11. Anreddy RNR (2018) Copper oxide nanoparticles induces oxidative stress and liver toxicity in rats following oral exposure. Toxicol Rep 5:903–904
12. Cholewińska E, Ognik K, Fotschki B, Zduńczyk Z, Juśkiewicz J (2018) Comparison of the effect of dietary copper nanoparticles and one copper(II) salt on the copper biodistribution and gastrointestinal and hepatic morphology and function in a rat model. PLoS ONE 13(5):e0197083
13. Bugata LSP, Pitta Venkata P, Gundu AR, Mohammed Fazlur R, Reddy UA, Kumar JM, Mahboob M (2019) Acute and subacute oral toxicity of copper oxide nanoparticles in female albino Wistar rats. J Appl Toxicol 39(5):702–716
14. Tang H, Xu M, Shi F, Ye G, Lv C, Luo J, Li Y (2018) Effects and mechanism of nano-copper exposure on hepatic cytochrome P450 enzymes in rats. Int J Mol Sci 19(7):2140
15. Distasi C, Ruffinatti FA, Dionisi M, Antoniotti S, Gilardino A, Croci G, Lovisolo D (2018) SiO_2 nanoparticles modulate the electrical activity of neuroendocrine cells without exerting genomic effects. Sci Rep 8(1):2760
16. Liu H, Lai W, Liu X, Yang H, Fang Y, Tian L, Xi Z (2021) Exposure to copper oxide nanoparticles triggers oxidative stress and endoplasmic reticulum (ER)-stress induced toxicology and apoptosis in male rat liver and BRL-3A cell. J Hazard Mater 401:123349
17. Ahmed FF, Ghareeb OA, Al-Bayti AAH (2022) Nephro defensive efficiency of cichorium intybus against toxicity caused by copper oxide nanoparticles. Pak J Med Health Sci 16(03):542–542
18. Mohammadyari A, Razavipour ST, Mohammadbeigi M, Negahdary M, Ajdary M (2014) Explore in-vivo toxicity assessment of copper oxide nanoparticle in Wistar rats. J Biol Today's world 3:124–128
19. De Jong WH, De Rijk E, Bonetto A, Wohlleben W, Stone V, Brunelli A, Cassee FR (2019) Toxicity of copper oxide and basic copper carbonate nanoparticles after short-term oral exposure in rats. Nanotoxicology 13(1):50–72
20. Bernhard S, Gregor L, Thomas R, Bruno S, Michael T, Zauner C, Georg-Christian F (2017) Acid-base disorders in liver disease. J Hepatol 67:66
21. Hinton DE, Segner H, Braunbeck T (2017) Toxic responses of the liver. In: Target organ toxicity in marine and freshwater teleosts. CRC Press, Boca Raton, pp 224–268
22. Zhao G, He F, Wu C, Li P, Li N, Deng J, Zhu G, Ren W, Peng Y (2018) Betaine in inflammation: mechanistic aspects and applications. Front Immunol 9:1070
23. Elsheikh NAH, Omer NA, Yi-Ru W, Mei-Qian K, Ilyas A, Abdurahim Y, Wang GL (2020) Protective effect of betaine against lead-induced testicular toxicity in male mice. J Androl 52(7):e13600
24. Lee EK, Jang EJ, Jung KJ, Kim DH, Yu BP, Chung HY (2013) Betaine attenuates lysophosphatidylcholine-mediated adhesion molecules in aged rat aorta: modulation of the nuclear factor-κB pathway. Exp Gerontol 48(5):517–524
25. Yang W, Huang L, Gao J, Wen S, Tai Y, Chen M, Huang Z, Liu R, Tang C, Li J (2017) Betaine attenuates chronic alcohol-induced fatty liver by broadly regulating hepatic lipid metabolism. Mol Med Rep 16(4):5225–5234
26. Alirezaei M, Jelodar G, Ghayemi Z, Mehr MK (2014) Antioxidant and methyl donor effects of betaine versus ethanol-induced oxidative stress in the rat liver. Comp Clin Path 23(1):161–168
27. Abdelazeim SA, Shehata NI, Aly HF, Shams SGE (2020) Amelioration of oxidative stress-mediated apoptosis in copper oxide nanoparticles-induced liver injury in rats by potent antioxidants. Sci Rep 10(1):1–14
28. Cullity BD (1976) Elements of X-ray diffraction, chapter 14, 3rd edn. Addison-Wesly, Singapore
29. Mohamed Mowafy S, Awad Hegazy A, Mandour DA, Salah Abd El-Fatah S (2021) Impact of copper oxide nanoparticles on the cerebral cortex of adult male albino rats and the potential protective role of crocin. Ultrastruct Pathol 45(4–5):307–318
30. Abdel-Daim MM, Abdellatief SA (2018) Attenuating effects of caffeic acid phenethyl ester and betaine on abamectin-induced hepatotoxicity and nephrotoxicity. Environ Sci Pollut Res 25(16):15909–15917
31. Hassan N, Rashad M, Elleithy E, Sabry Z, Ali G, Elmosalamy S (2023) L-Carnitine alleviates hepatic and renal mitochondrial-dependent apoptotic progression induced by letrozole in female rats through modulation of Nrf-2, Cyt c and CASP-3 signaling. Drug Chem Toxicol 46:1–12
32. Hashim AR, Bashir DW, Yasin NA, Rashad MM, El-Gharbawy SM (2022) Ameliorative effect of N-acetylcysteine on the testicular tissue of adult male albino rats after glyphosate-based herbicide exposure. J Biochem Mol Toxicol 36(4):e22997
33. Hesham A, Abass M, Abdou H, Fahmy R, Rashad MM, Abdallah AA, Mossallem W, Rehan IF, Elnagar A, Zigo F (2023) Ozonated saline intradermal injection: promising therapy for accelerated cutaneous wound healing in diabetic rats. Front Vet Sci 10:66
34. Elmosalamy SH, Elleithy EM, Ahmed ZSO, Rashad MM, Ali GE, Hassan NH (2022) Dysregulation of intraovarian redox status and steroidogenesis pathway in letrozole-induced PCOS rat model: a possible modulatory role of l-Carnitine. BJBAS 11(1):1–15

35. Bashir DW, Rashad MM, Ahmed YH, Drweesh EA, Elzahany EA, Abou-El-Sherbini KS, Elleithy EM (2021) The ameliorative effect of nanoselenium on histopathological and biochemical alterations induced by melamine toxicity on the brain of adult male albino rats. Neurotoxicology 86:37–51
36. Ahmed YH, El-Naggar ME, Rashad MM, Youssef AM, Galal MK, Bashir DW (2022) Screening for polystyrene nanoparticle toxicity on kidneys of adult male albino rats using histopathological, biochemical, and molecular examination results. Cell Tissue Res 388(1):149–165
37. Bancroft JD, Gamble M (2013) Theories and practice of histological techniques. NY Lond Madrid Churchil Livingstone 7(12):2768–2773
38. Hashim AR, Bashir DW, Yasin NA, Galal MK, El-Gharbawy SM (2021) Ameliorative effect of N-acetylcysteine against glyphosate-induced hepatotoxicity in adult male albino rats: histopathological, biochemical, and molecular studies. Environ Sci Pollut Res 28:42275–42289
39. Fuentes-Santamaría V, Alvarado JC, Gabaldón-Ull MC, Manuel Juiz J (2013) Upregulation of insulin-like growth factor and interleukin 1β occurs in neurons but not in glial cells in the cochlear nucleus following cochlear ablation. J Comp Neurol 521(15):3478–3499
40. Noshy PA, Yasin NA, Rashad MM, Shehata AM, Salem FM, El-Saied EM, Mahmoud MY (2023) Zinc nanoparticles ameliorate oxidative stress and apoptosis induced by silver nanoparticles in the brain of male rats. Neurotoxicology 95:193–204
41. Hashim AR, Bashir DW, Rashad E, Galal MK, Rashad MM, Khalil HMA, Deraz NM, Drweesh EA, El-Gharbawy SM (2024) Neuroprotective assessment of betaine against copper oxide nanoparticle-induced neurotoxicity in the brains of albino rats: a histopathological, neurochemical, and molecular investigation. ACS Chem Neurosci 15(8):1684–1701
42. Ganesan S, Anaimalai Thirumurthi N, Raghunath A, Vijayakumar S, Perumal E (2016) Acute and sub-lethal exposure to copper oxide nanoparticles causes oxidative stress and teratogenicity in zebrafish embryos. J Appl Toxicol 36(4):554–567
43. Heidari R, Niknahad H, Sadeghi A, Mohammadi H, Ghanbarinejad V, Ommati MM, Hosseini A, Azarpira N, Khodaei F, Farshad O (2018) Betaine treatment protects liver through regulating mitochondrial function and counteracting oxidative stress in acute and chronic animal models of hepatic injury. Biomed Pharmacother 103:75–86
44. Zhang A, Sun H, Wang X (2013) Recent advances in natural products from plants for treatment of liver diseases. EJMECH 63:570–577
45. Poon W, Kingston BR, Ouyang B, Ngo W, Chan WC (2020) A framework for designing delivery systems. Nat Nanotechnol 15(10):819–829
46. Lu R, Yang D, Cui D, Wang Z, Guo L (2012) Egg white-mediated green synthesis of silver nanoparticles with excellent biocompatibility and enhanced radiation effects on cancer cells. Int J Nanomed 66:2101–2107
47. Chang C, Meikle TG, Su Y, Wang X, Dekiwadia C, Drummond CJ, Conn CE, Yang Y (2019) Encapsulation in egg white protein nanoparticles protects anti-oxidant activity of curcumin. Food Chem 280:65–72
48. Sabouri Z, Akbari A, Hosseini HA, Khatami M, Darroudi M (2020) Egg white-mediated green synthesis of NiO nanoparticles and study of their cytotoxicity and photocatalytic activity. Polyhedron 178:114351
49. Kargar H, Ghazavi H, Darroudi M (2015) Size-controlled and bio-directed synthesis of ceria nanopowders and their in vitro cytotoxicity effects. Ceram Int 41(3):4123–4128
50. Tirado-Guizar A, Rodriguez-Gattorno G, Paraguay-Delgado F, Oskam G, Pina-Luis GE (2017) Eco-friendly synthesis of egg-white capped silver nanoparticles for rapid, selective, and sensitive detection of Hg(II). MRS Commun 7(3):695–700
51. Cittrarasu V, Kaliannan D, Dharman K, Maluventhen V, Easwaran M, Liu WC, Balasubramanian B, Arumugam M (2021) Green synthesis of selenium nanoparticles mediated from Ceropegia bulbosa Roxb extract and its cytotoxicity, antimicrobial, mosquitocidal and photocatalytic activities. Sci Rep 11(1):1–15
52. Chen W, Li X, Cheng H, Zhan X, Xia W (2023) Synthesis, characterization, and anticancer activity of protamine sulfate stabilized selenium nanoparticles. Int Food Res J 164:112435
53. Chuntonov L, Kumar R, Kuroda DG (2014) Non-linear infrared spectroscopy of the water bending mode: direct experimental evidence of hydration shell reorganization. PCCP 16(26):13172–13181
54. Betancourt-Galindo R, Reyes-Rodriguez P, Puente-Urbina B, Avila-Orta C, Rodríguez-Fernández O, Cadenas-Pliego G, Lira-Saldivar R, García-Cerda L (2014) Synthesis of copper nanoparticles by thermal decomposition and their antimicrobial properties. J Nanomater 66:10
55. Reddy KR (2017) Green synthesis, morphological and optical studies of CuO nanoparticles. J Mol Struct 1150:553–557
56. Amaliyah S, Pangesti DP, Masruri M, Sabarudin A, Sumitro SB (2020) Green synthesis and characterization of copper nanoparticles using *Piper retrofractum* Vahl extract as bioreductor and capping agent. Heliyon 6(8):66
57. Debbichi L, Marco de Lucas M, Pierson J, Kruger P (2012) Vibrational properties of CuO and Cu_4O_3 from first-principles calculations, and Raman and infrared spectroscopy. J Phys Chem A 116(18):10232–10237
58. Goldstein H, Kim DS, Peter YY, Bourne L, Chaminade J, Nganga L (1990) Raman study of CuO single crystals. Phys Rev B 41(10):7192
59. Xu J, Ji W, Shen Z, Li W, Tang S, Ye X, Jia D, Xin X (1999) Raman spectra of CuO nanocrystals. J Raman Spectrosc 30(5):413–415
60. Yasin NA, El-Naggar ME, Ahmed ZSO, Galal MK, Rashad MM, Youssef AM, Elleithy EM (2022) Exposure to polystyrene nanoparticles induces liver damage in rat via induction of oxidative stress and hepatocyte apoptosis. Environ Toxicol Pharmacol 94:103911
61. Contreras-Zentella ML, Hernández-Muñoz R (2016) Is liver enzyme release really associated with cell necrosis induced by oxidant stress? Oxid Med Cell Longev 12:1–12
62. Tang H, Xu M, Luo J, Zhao L, Ye G, Shi F, Lv C, Chen H, Wang Y, Li Y (2019) Liver toxicity assessments in rats following sub-chronic oral exposure to copper nanoparticles. Environ Sci Eur 31(1):1–14
63. Abdel-Azeem AM, Abdel-Rehiem ES, Farghali AA, Khidr FK, Abdul-Hamid M (2023) Comparative toxicological evaluations of novel forms nano-pesticides in liver and lung of albino rats. J Mol Histol 54(2):157–172
64. Sutunkova MP, Ryabova YV, Minigalieva IA, Bushueva TV, Sakhautdinova RR, Bereza IA, Shaikhova DR, Amromina AM, Chemezov AI, Shelomencev IG (2023) Features of the response to subchronic low-dose exposure to copper oxide nanoparticles in rats. Sci Rep 13(1):11890
65. Ingle AP, Duran N, Rai M (2014) Bioactivity, mechanism of action, and cytotoxicity of copper-based nanoparticles: a review. Appl Microbiol Biotechnol 98:1001–1009
66. Fu PP, Xia Q, Hwang HM, Ray PC, Yu H (2014) Mechanisms of nanotoxicity: generation of reactive oxygen species. JFDA 22(1):64–75
67. Genestra M (2007) Oxyl radicals, redox-sensitive signalling cascades and antioxidants. Cell Signal 19(9):1807–1819
68. Gabay C, Lamacchia C, Palmer G (2010) IL-1 pathways in inflammation and human diseases. Nat Rev J Rheumatol 6(4):232–241
69. Dumoulin FL, Leifeld L, Honecker U, Sauerbruch T, Spengler U (1999) Intrahepatic expression of Interleukin-1β and tumor necrosis factor—α in chronic hepatitis C. J Infect Dis 180(5):1704–1708
70. Trickler WJ, Lantz SM, Schrand AM, Robinson BL, Newport GD, Schlager JJ, Paule MG, Slikker W, Biris AS, Hussain S (2012) Effects of copper nanoparticles on rat cerebral microvessel endothelial cells. Nanomed J 7(6):835–846
71. Zhai Y, Tang H, Zhang Q, Peng Y, Zhao L, Zhang B, Yang Y, Ma J, Zhu J, Zhang D (2023) The protective effect of *Lycium barbarum* betaine and effervescent tablet against carbon tetrachloride-induced acute liver injury in rats. Nat Prod Commun 18(3):1934578X231161419
72. Arumugam MK, Paal MC, Donohue TM Jr, Ganesan M, Osna NA, Kharbanda KK (2021) Beneficial effects of betaine: a comprehensive review. J Biol 10(6):456
73. Kanbak G, Akyüz F, Inal M (2001) Preventive effect of betaine on ethanol-induced membrane lipid composition and membrane ATPases. Arch Toxicol 75:59–61
74. Özkoç M, Karimkhani H, Kanbak G, Burukoğlu Dönmez D (2020) Hepatotoxicity and nephrotoxicity following long-term prenatal exposure of paracetamol in the neonatal rat: Is betaine protective? Turk J Biochem 45(1):99–107
75. Ilyas A, Wijayasinghe YS, Khan I, El Samaloty NM, Adnan M, Dar TA, Poddar NK, Singh LR, Sharma H, Khan S (2022) Implications of trimethylamine *N*-oxide (TMAO) and betaine in human health: beyond being osmoprotective compounds. Front Mol Biosci 9:964624
76. Hasanzadeh-Moghadam M, Khadem-Ansari MH, Farjah GH, Rasmi Y (2018) Hepatoprotective effects of betaine on liver damages followed by myocardial infarction. Vet Res Forum 9(2):129
77. Ghonimi WA, Alferah DN, El-Shetry ES (2022) Hepatic and renal toxicity following the injection of copper oxide nanoparticles (CuO NPs) in mature male Westar rats: histochemical and caspase 3 immunohistochemical reactivities. Environ Sci Pollut Res 29(54):81923–81937

78. Pérez-Iglesias JM, Franco-Belussi L, Moreno L, Tripole S, de Oliveira C, Natale GS (2016) Effects of glyphosate on hepatic tissue evaluating melanomacrophages and erythrocytes responses in neotropical anuran *Leptodactylus latinasus*. Environ Sci Pollut Res 23:9852–9861
79. Tohamy HG, El Okle OS, Goma AA, Abdel-Daim MM, Shukry M (2022) Hepatorenal protective effect of nano-curcumin against nano-copper oxide-mediated toxicity in rats: behavioral performance, antioxidant, anti-inflammatory, apoptosis, and histopathology. Life Sci 292:120296
80. Cheville NF (2009) Ultrastructural pathology: the comparative cellular basis of disease. Wiley, New York
81. Elhussainy E, El-Shourbagy S (2014) Protective effect of multivitamin complex on copper oxide nanoparticles (nanoCuO) induced toxicity in rats. Bull ESPS 34(2):404–418
82. Stevens A, Lowe J, Young H (2004) Anatomy pathology, 4th edn. Atlas de Whlater, De Boeck, Bruxelle
83. Abdel Hameed T (2004) Light and electron microscopic studies on the effect of orally-adminstered formalin on liver and kidney of guinea pig. JOBAZ 45(C):203–224
84. Cho WS, Duffin R, Bradley M, Megson IL, MacNee W, Lee JK, Jeong J, Donaldson K (2013) Predictive value of in vitro assays depends on the mechanism of toxicity of metal oxide nanoparticles. Part Fibre Toxicol 10(1):1–15
85. Fahmy B, Cormier SA (2009) Copper oxide nanoparticles induce oxidative stress and cytotoxicity in airway epithelial cells. In Vitro Toxicol 23(7):1365–1371
86. Marc J, Mulner-Lorillon O, Boulben S, Hureau D, Durand G, Bellé R (2002) Pesticide roundup provokes cell division dysfunction at the level of CDK1/cyclin B activation. Chem Res Toxicol 15(3):326–331
87. Privalova LI, Katsnelson BA, Loginova NV, Gurvich VB, Shur VY, Valamina IE, Makeyev OH, Sutunkova MP, Minigalieva IA, Kireyeva EP (2014) Subchronic toxicity of copper oxide nanoparticles and its attenuation with the help of a combination of bioprotectors. Int J Mol Sci 15(7):12379–12406
88. Sato K, Marzioni M, Meng F, Francis H, Glaser S, Alpini G (2019) Ductular reaction in liver diseases: pathological mechanisms and translational significances. J Hepatol 69(1):420–430
89. Alirezaei M, Jelodar G, Niknam P, Ghayemi Z, Nazifi S (2011) Betaine prevents ethanol-induced oxidative stress and reduces total homocysteine in the rat cerebellum. Physiol J Biochem 67:605–612
90. Ganesan B, Buddhan S, Anandan R, Sivakumar R, AnbinEzhilan R (2010) Antioxidant defense of betaine against isoprenaline-induced myocardial infarction in rats. Mol Biol Rep 37:1319–1327
91. Veskovic M, Mladenovic D, Milenkovic M, Tosic J, Borozan S, Gopcevic K, Labudovic-Borovic M, Dragutinovic V, Vucevic D, Jorgacevic B (2019) Betaine modulates oxidative stress, inflammation, apoptosis, autophagy, and Akt/mTOR signaling in methionine-choline deficiency-induced fatty liver disease. Eur J Pharmacol 848:39–48

Publisher's Note